10868 *Inorg. Chem.* **2009**, *48*, 10868–10870
DOI: 10.1021/ic9013703

Inorganic Chemistry
Communication

Using the Antenna Effect as a Spectroscopic Tool: Photophysics and Solution Thermodynamics of the Model Luminescent Hydroxypyridonate Complex $[Eu^{III}(3,4,3\text{-LI}(1,2\text{-HOPO}))]^{-}$

Rebecca J. Abergel,[†] Anthony D'Aléo,[†] Clara Ng Pak Leung,[†] David K. Shuh,[†] and Kenneth N. Raymond*[,†,‡]

[†]*Chemical Sciences Division, Lawrence Berkeley National Laboratory, Berkeley, California 94720, and*
[‡]*Department of Chemistry, University of California, Berkeley, California 94720-1460*

Received July 13, 2009

Although widely used in bioassays, the spectrofluorimetric method described here uses the antenna effect as a tool to probe the thermodynamic parameters of ligands that sensitize lanthanide luminescence. The Eu^{3+} coordination chemistry, solution thermodynamic stability, and photophysical properties of the spermine-based hydroxypyridonate octadentate chelator 3,4,3-LI(1,2-HOPO) are reported. The complex $[Eu^{III}(3,4,3\text{-LI}(1,2\text{-HOPO}))]^{-}$ luminesces with a long lifetime (805 μs) and a quantum yield of 7.0% in aqueous solution, at pH 7.4. These remarkable optical properties were exploited to determine the high (and proton-independent) stability of the complex ($\log \beta_{110} = 20.2(2)$) and to define the influence of the ligand scaffold on the stability and photophysical properties.

The high-affinity bidentate hydroxypyridonate (HOPO) metal-chelating groups are related to microbial siderophores: they combine the structural features of hydroxamic acids with the electronic properties of catechols. The 6-amide derivative of 1-hydroxy-pyridin-2-one (1,2-HOPO) has been linked to multiple polyamine scaffolds through amide coupling, to form multidentate ligand structures used for a variety of applications such as actinide (An) and iron chelation,[1,2] MRI contrast enhancement,[3] and lanthanide (Ln) luminescence sensitization.[4] The coordination chemistry properties of these ligands can be fine-tuned by systematic modifications of the denticity, geometry, and acidity of the backbone. Octadentate ligands, each incorporating four 1,2-HOPO functionalities, are known to strongly bind Ln(III), An(III), and An(IV) and to act as antennae that sensitize the emission of Eu(III).[1,5] The backbone geometry of the ligand must affect the thermodynamic stability and photophysical properties of the corresponding Ln and An complexes, but this has not been investigated in a systematic way. Although the octadentate ligand 3,4,3-LI(1,2-HOPO) (**1**, Figure 1) is composed of 1,2-HOPO units linked to a central linear spermine scaffold and has shown potential as a therapeutic Pu(IV) and Am(III) chelator,[1] the branched tetrapodal ligand H(2,2)-1,2-HOPO (**2**, Figure 1) has been studied for its ability to form a highly stable luminescent Eu(III) complex that contains a molecule of water in the inner coordination sphere at physiological pH.[5] The work presented herein probes the coordination chemistry and photophysical properties of the Gd(III) and Eu(III) complexes of **1**, showing that the geometry of the ligand scaffold strongly affects the inner coordination sphere of the metal ion and consequently its emissive properties. In addition, the Eu luminescence sensitization properties of the antenna ligand **1** are used as a spectroscopic tool to determine the solution thermodynamic stability of the corresponding metal complex, which provides a new method for the accurate determination of these thermodynamic parameters.

All photophysical properties were measured in buffered aqueous solutions at pH 7.4 and relevant parameters are summarized in Table 1. The electronic absorption spectrum of $[Eu^{III}(\mathbf{1})]^{-}$ (Figure 2) shows an absorption maximum due to $\pi-\pi^*$ transitions at $\lambda_{max} = 315$ nm ($\varepsilon = 17\,700$ M^{-1} cm^{-1}). The lowest absorption transition is blue shifted and has a lower molar absorption coefficient than the one of $[Eu^{III}(\mathbf{2})]^{0}$ ($\lambda_{max} = 343$ nm, $\varepsilon = 18\,200$ $M^{-1}cm^{-1}$,[5] Figure 2). The shift toward higher energies is attributed to the different ligand scaffolds: the four protonated amide nitrogen atoms in the molecular structure of **2** can form hydrogen bonds with the hydroxyl groups from the pyridinone rings, thereby stabilizing the first singlet excited state of the corresponding europium complex, whereas the backbone of **1** only contains two protonated amide nitrogen atoms yielding a complex with a singlet excited state slightly higher in energy, and a shoulder at lower energy on the main absorption peak.

The Gd(III) complex of **1** was prepared in situ, to determine the ligand centered triplet excited state energy. Because

*To whom correspondence should be addressed. E-mail: raymond@socrates.berkeley.edu. Fax: (510) 486 5283.

(1) Durbin, P. W. *Health Phys.* **2008**, *95*, 465–492.
(2) Scarrow, R. C.; Riley, P. E.; Abu-Dari, K.; White, D. L.; Raymond, K. N. *Inorg. Chem.* **1985**, *24*, 954–967.
(3) Werner, E. J.; Datta, A.; Jocher, C. J.; Raymond, K. N. *Angew. Chem., Int. Ed.* **2008**, *47*, 8568–8580.
(4) Moore, E. G.; Samuel, A. P. S.; Raymond, K. N. *Acc. Chem. Res.* **2009**, *42*, 542–552.
(5) Moore, E. G.; Jocher, C. J.; Xu, J.; Werner, E. J.; Raymond, K. N. *Inorg. Chem.* **2007**, *46*, 5468–5470.

 Published on Web 11/10/2009 © 2009 American Chemical Society

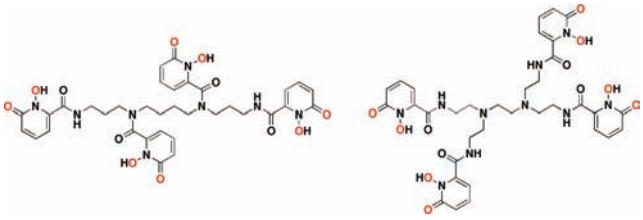

Figure 1. Structures of the octadentate hydroxypyridonate ligands 3,4,3-LI(1,2-HOPO) (**1**, left) and H(2,2)-1,2-HOPO (**2**, right); the metal-coordinating oxygen atoms are indicated in red.

Table 1. Summary of Photophysical Parameters for $[Eu^{III}(\mathbf{1})]^{-a}$

λ_{max}, ε_{max} (nm, M^{-1} cm^{-1})	315, 17700	τ_{rad} (μs)	1860
τ_{obs} {H_2O} (μs)	805 ± 81	k_{rad} (s^{-1})	540
τ_{obs} {D_2O} (μs)	1120 ± 112	k_{nonrad} (s^{-1})	705
Φ_{tot} (H_2O)	0.070 ± 0.007	η^{Eu}	0.432
q	0.1 ± 0.1	η_{sens}	0.162

[a] The uncertainties were determined from the standard deviation between three independent experiments performed in aqueous buffered solutions (TRIS, pH 7.4).

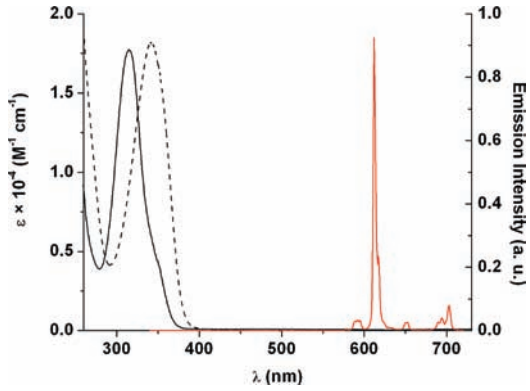

Figure 2. Electronic absorption (solid, left) and normalized steady-state emission spectra (solid, right, λ_{exc} = 325 nm) of $[Eu^{III}(\mathbf{1})]^-$, and electronic absorption spectrum (dash) of $[Eu^{III}(\mathbf{2})]^0$, in 0.1 M TRIS buffer (pH 7.4).

the Gd^{3+} ion exhibits a size and atomic weight similar to Eu^{3+} but lacks an appropriately positioned electronic acceptor level, the phosphorescence of the ligand can be observed by luminescence measurements in a solid matrix (1:3 (v/v) MeOH:EtOH) at 77 K. Upon cooling to 77 K, the spectrum of $[Gd^{III}(\mathbf{1})]^-$ reveals an intense unstructured emission band from 400 to 570 nm (see Figure S1 in the Supporting Information), assigned to phosphorescence from the ligand T_1 excited state. The lowest T_1 excited state energy was estimated by spectral deconvolution of the 77 K luminescence signal into several overlapping Gaussian functions.[6] The resulting T_1 energy was calculated at 24 390 cm^{-1}, which is higher than the values found for other 1,2-HOPO derivatives ($T_1 \approx$ 19 500−21 500 cm^{-1}),[4] and the energy gap between T_1 and the $^5D_1$ accepting state of Eu(III) was determined at 5360 cm^{-1}, a value larger than that found for **2**, implying that the energy transfer efficiency of $[Eu^{III}(\mathbf{1})]^-$ should be less efficient. This increase of the triplet excited state energy corresponds with the increase of the singlet excited state energy determined by UV−visible absorption spectroscopy and can also be attributed to the absence of two protonated amide nitrogen (destabilizing the triplet excited state as compared to that of $[Eu^{III}(\mathbf{2})]^0$).

The luminescence spectrum of $[Eu^{III}(\mathbf{1})]^-$ displays the characteristic features of Eu^{III}(1,2-HOPO) complexes; the very intense $^5D_0 \rightarrow {}^7F_2$ hypersensitive transition results in almost pure red luminescence (λ_{em} = 612 nm, Figure 2). The luminescence quantum yield of $[Eu^{III}(\mathbf{1})]^-$ in aqueous solution (pH 7.4), Φ_{tot} = 7.0%, is 2-fold higher than that of $[Eu^{III}(\mathbf{2})]^0$ (3.6%),[5] thus $[Eu^{III}(\mathbf{1})]^-$ is much brighter than $[Eu^{III}(\mathbf{2})]^0$ (the brightness is defined as the product of molar absorption coefficient and luminescence quantum yield). The optical properties of the 3,4,3-LI backbone are superior to those of the H(2,2) backbone at high energy, up to 337 nm, and are slightly inferior at lower energies (see Figure S2 in the Supporting Information).

Corresponding time-resolved analysis of $[Eu^{III}(\mathbf{1})]^-$ luminescence, measured at 612 nm in H_2O and D_2O, revealed monoexponential decays with decay times of ca. 805 μs and ca. 1120 μs, respectively, which are slightly longer than the typical lifetimes determined for bis-tetradentate Eu^{III}(1,2-HOPO) complexes.[6,7] Using the improved Horrocks equation,[8] the number of inner sphere water molecules on the $[Eu^{III}(\mathbf{1})]^-$ complex was determined as q = 0.1 ± 0.1, essentially zero. In contrast to complexes formed with H(2,2) ligand derivatives,[5] the 3,4,3-LI linear backbone promotes the formation of a Eu(III) complex with no inner sphere water molecule.

To investigate in detail further particularities of the sensitization process by the linear ligand **1**, we determined the kinetic parameters.[9,10] The sensitization efficiency, η_{sens}, defined as the product of the efficiency of the energy transfer, η_{ET}, and the intersystem crossing efficiency, η_{ISC} was determined using the equation: $\Phi_{Tot} = \eta_{Eu} \times \eta_{sens}$ where η_{Eu} is the metal centered efficiency. The radiative decay rate, k_{rad}, of $[Eu^{III}(\mathbf{1})]^-$ is higher than that of $[Eu^{III}(\mathbf{2})]^0$ (538 vs 333 s^{-1}), and the nonradiative decay rate, k_{nonrad}, is much lower for the linear complex than for the branched complex with values of 705 and 1750 s^{-1}, respectively. This result reflects the absence of water molecule in the inner sphere of $[Eu^{III}(\mathbf{1})]^-$, inducing a decrease of the quenching by OH vibrations. Consequently, the metal centered luminescence efficiency is higher for $[Eu^{III}(\mathbf{1})]^-$ than for $[Eu^{III}(\mathbf{2})]^0$ (43.2% vs. 16.0%), although the sensitization efficiency, η_{sens}, is lower (16.2% *vs* ca. 22.5%). The intersystem crossing and the energy transfer are therefore affected when using the 3,4,3-LI backbone, which limits the corresponding luminescence quantum yield to 7.0%. These values emphasize the important trade off existing between the sensitization and metal efficiency of the Eu^{III} complexes.

The protonation constants of **1** were determined by potentiometric titrations, and four protonation equilibria (Table 2) were assigned to sequential removal of one proton from each of the four 1,2-HOPO units. The overall basicity of **1** (quantified from the sum of the log K_a values associated to only those protonation steps that result in the neutral ligand species,[11] $\Sigma \log K_a$ = 21.2) is increased when compared to the branched ligand **2** ($\Sigma \log K_a$ = 18.9).[5] Initial attempts were

(6) Moore, E. G.; Xu, J.; Jocher, C. J.; Castro-Rodriguez, I.; Raymond, K. N. *Inorg. Chem.* **2008**, *47*, 3105–3118.

(7) D'Aléo, A.; Xu, J.; Moore, E. G.; Jocher, C. J.; Raymond, K. N. *Inorg. Chem.* **2008**, *47*, 6109–6111.

(8) Supkowski, R. M.; Horrocks, W. D. *Inorg. Chim. Acta* **2002**, *340*, 44–48.

(9) Beeby, A.; Bushby, L. M.; Maffeo, D.; Williams, J. A. G. *J. Chem. Soc., Dalton Trans.* **2002**, 48–54.

(10) Werts, M. H. V.; Jukes, R. T. F.; Verhoeven, J. W. *Phys. Chem. Chem. Phys.* **2002**, *2002*, 1542–1548.

(11) Kumar, K.; Tweedle, M. F.; Malley, M. F.; Gougoutas, J. Z. *Inorg. Chem.* **1995**, *34*, 6472–6480.

Table 2. Protonation and Eu Complex Formation Constants for Ligand **1**[a]

species	*m*, *l*, *h*	log β_{mlh}
LH	0, 1, 1	6.64(1)
LH_2	0, 1, 2	12.32(1)
LH_3	0, 1, 3	17.33(1)
LH_4	0, 1, 4	21.20(1)
EuL	1, 1, 0	20.2(2)
EuLH	1, 1, 1	24.8(1)
pEu^{III}[b]		21.1(1)
pEu^{III}[c]		21.3(2)

[a] The figures in parentheses give the uncertainties determined from the standard deviation between three independent titrations; pEu^{III} values indicate the negative log value of the free Eu(III) concentration at pH 7.4, 1 μM [Eu], and 10 μM [**1**]. [b] Value calculated from protonation and complex formation constants. [c] Value determined by direct competition against DTPA at pH 7.4.

made to determine the Eu(III) affinity of **1** by direct spectrophotometric titration (Figure S3). However, few changes occur in the UV−visible absorption of the complex over the pH range 3.0−8.0, limiting accurate spectral deconvolution and data refinement. The Eu^{3+} complexation of **1** was thus studied by spectrofluorimetric titration: a solution containing an equimolar ratio of Eu and **1** was divided into separate aliquots, and base was added to each sample to give a pH range from 2.2 to 9.5. After a 24 h equilibration time, each emission spectrum (λ_{exc} = 325 nm) and pH was recorded and analyzed to ascertain the proton-independent stability constant ($K_f = \beta_{110} = 10^{20.2(2)}$) and protonation constant ($K_a = 10^{4.6(1)}$) of the corresponding europium complex (Table 2). In contrast to previous studies,[12] the present method relies on the sensitization of the Eu luminescence by the excited ligand rather than on the emission resulting from direct excitation of the metal ion. Upon acidification, the luminescence of the solution decreases (Figure 3), corresponding to the disappearance of the emissive species $[Eu^{III}(\mathbf{1})]^-$ and the formation of the protonated complex $[Eu^{III}(\mathbf{1H})]^0$. In addition, only a single monoexponential decay lifetime (805 μs ± 10%), corresponding to the parent complex $[Eu^{III}(\mathbf{1})]^-$, was detected through time-resolved measurements of the titration samples.

The conditional stability constant pEu^{III} could then be calculated as a function of pH for a standard set of conditions (see Figure S4 in the Supporting Information, initial concentrations: [Eu] = 1×10^{-6} M, [L] = 1×10^{-5} M), to allow comparisons between **1** and other ligands of varying denticity and/or acidity. Both **1** ($pEu^{III}_{7.4}$ = 21.1(1)) and **2** ($pEu^{III}_{7.4}$ = 21.2) exhibit similar affinities for Eu(III), not only at pH 7.4, but over the pH range 2.0−10, despite the differences in ligand acidity and water coordination of the corresponding complexes. To validate the use of this spectrofluorimetric method,

(12) Wu, S. L.; Horrocks, W. D. *J. Chem. Soc., Dalton Trans.* **1997**, 1497–1502.

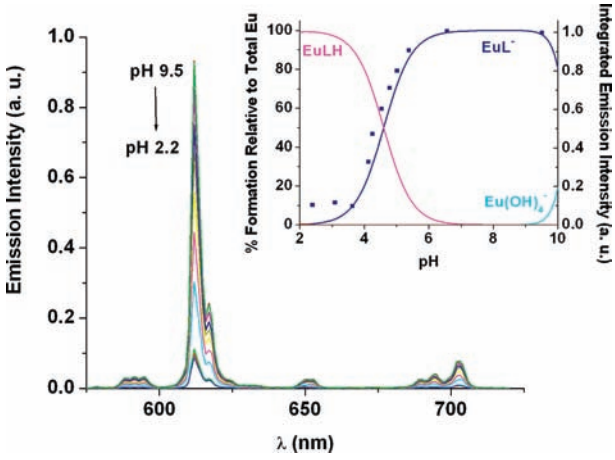

Figure 3. Spectrofluorimetric titration of $[Eu^{III}(\mathbf{1})]^-$ ($[Eu^{3+}]$ = [**1**] = 0.01 mM, 0.1 M KCl, 0.2 mM Hepes, 0.2 mM Mes, 25.0 °C, λ_{exc} = 325 nm). Inset: Normalized integration of the emission spectra (data points) and calculated speciation diagram corresponding to the titration conditions (solid lines).

we verified the affinity of **1** for Eu(III) via direct competition against diethylenetriaminepentaacetic acid (DTPA) at pH 7.4, following a previously described method (see Figures S5 and S6 in the Supporting Information, Table 2).[5]

Although the linear spermine-based 1,2-HOPO ligand **1** and the tetrapodal ligand **2** both exhibit similar affinities for Eu(III), the photophysical properties of the resulting complexes differ significantly. In contrast to $[Eu^{III}(\mathbf{2})]^0$, the high quantum yield of the bright complex $[Eu^{III}(\mathbf{1})]^-$ comes mainly from its high metal-centered luminescence efficiency and from the lack of an inner-sphere water molecule. The remarkable luminescence properties of $[Eu^{III}(\mathbf{1})]^-$ were used to design a direct method of stability constant determination. This method will be applied to other ligand systems that sensitize lanthanide and actinide luminescence.

Acknowledgment. This work was supported by the National Institutes of Health (Grant AI074065-01), the Director, Office of Science, Office of Basic Energy Sciences, the Division of Chemical Sciences, Geosciences, and Biosciences of the U.S. Department of Energy at LBNL under Contract No. DE-AC02-05CH11231. The authors thank Dr. Jide Xu for providing the ligands and Prof. Gilles Muller (San Jose State University) for the use of a low-temperature time-resolved luminescence spectrometer. This technology is licensed to Lumiphore, Inc., in which some of the authors have a financial interest.

Supporting Information Available: Detailed experimental procedures and spectral data (PDF). This material is available free of charge via the Internet at http://pubs.acs.org.